Desalination and Water Treatment
www.deswater.com
doi: 10.1080/19443994.2015.1082945

57 (2016) 16970–16980
August

Taylor & Francis
Taylor & Francis Group

Adsorption behaviour of congo red by cellulose/chitosan hydrogel beads regenerated from ionic liquid

Manfeng Li[a], Zhaomei Wang[a,b,*], Bingjie Li[a]

[a]*College of Light Industry & Food Science, South China University of Technology, Guangzhou 510640, China, Tel. +86 18814123312; email: manfengli7@126.com (M. Li), Tel. +86 020 87113843; email: wangzm@scut.edu.cn (Z. Wang), Tel. +86 13570066007; email: 942254135@qq.com (B. Li)*
[b]*State Key Laboratory of Pulp and Paper Engineering, South China University of Technology, Guangzhou 510640, China*

Received 2 March 2015; Accepted 8 August 2015

ABSTRACT

A cellulose/chitosan hydrogel bead was prepared by extruding and regenerating the blends from ionic liquid 1-ethyl-3-methylimidazolium acetate ([Emim]Ac) in ethanol. FT-IR, scanning electron microscopy (SEM) and X-ray powder diffraction techniques were used to prove the successful blending of both natural polymers (cellulose and chitosan). Brunauer–Emmet–Teller surface area and pore diameter analysis showed that the beads were nanoporous with pores measuring from 10 to 20 nm. Batch adsorption experiments demonstrated that the bead had a maximum adsorption capacity of 40 mg/g for congo red (CR) dye removal from aqueous solutions, which was more efficient than the most reported natural biosorbents. The CR adsorption capacity at equilibrium was related to initial CR concentration, dosage of beads and pH values of the CR solution. When the initial concentration of CR was 30 mg/L, and the adsorbent dosage was 2.0 g/L, the equilibrium of adsorption was reached within 115 min with the removal rate of 89.6%. The Langmuir model represented the adsorption isotherm data and the experimental results followed a pseudo-second-order rate model, indicating that intraparticle diffusion dominated the adsorption process. The cellulose/chitosan hydrogel beads can be used as an efficient adsorbent for dye contaminant removal from wastewater.

Keywords: Adsorption; Cellulose; Chitosan; Hydrogel beads; Congo red

1. Introduction

Dyes and pigments are discharged by many processes in the textile, printing, rubber, plastic, cosmetic, leathers, pharmaceutical and food industries. Consequently, coloured wastewater is generated [1]. Even a small amount of the dye discharged in wastewater has a serious environmental impact as well as causing damage to human health [2]. It was therefore necessary to find an efficient, green and low-cost method to remove such colouring pollutants from wastewaters for the sake of environmental protection. To remove congo red (CR) dye contamination from effluent, various methods have been tried, including sonochemical treatment [3], electrochemical treatment [3,4], photocatalytic oxidation [5,6] and adsorption [7,8]. However, these technologies vary in their effectiveness, complexity and environmental impact [9]. Among them, adsorption technology is a

*Corresponding author.

more attractive and promising method of dye removal with advantages of simplicity, easy recovery, efficiency, ready availability and the ability to reuse the absorbent.

Recently, finding low-cost, effective materials to remove different colour contaminants has attracted growing research interest. In particular, eco-friendly, low-cost, biocompatible agents have attracted the most attention. Cellulose is considered the most abundant biopolymer in the world, and is renewable, biocompatible and biodegradable. Chitosan, a linear biopolymer of glucosamine, is an effective adsorbent for dyes and metal ions due to its high content of amino and hydroxyl functional groups [10]. It is the second most abundant natural polymer on earth [11] and has been used in various industries, including: agriculture, pharmaceuticals, biomedical engineering and environmental protection [12,13]. Chitosan hydrogel beads have been prepared by lowering the degree of crystallinity by the way of forming a gel for the purpose of enhancing the adsorption capacity of chitosan. However, because hydrogel beads were of low mechanical strength and promoted acidic conditions, several techniques have been tried to enhance the commercial application of cellulose/chitosan beads using chemical cross-linking with cross-linking agents on their surface. Jin and Bai have investigated the adsorption capacity of chitosan/polyvinyl alcohol (PVA) hydrogel beads for lead removal and discovered that the mechanical strength of the hydrogel beads was improved by blending PVA with the chitosan [14]. Cellulose has special mechanical and physical characteristics suitable for various uses [15]. Cellulose films and beads have been used to remove hazardous azo dyes [16,17] and heavy metals [18–21]. Also, cellulose gel shows a good affinity with synthetic polymers, such as cellulose gel-based polymeric nanocomposites, because of its hydrophobic surface [22]. Nevertheless, its application has been limited because of its compact and inactive molecular structure. It should be modified to improve its hydrophilicity as an adsorbent to remove dye contaminants. So far, there has been no report in the literatures about the preparation of cellulose/chitosan composite bead and study of the adsorption dye ability for dye removal.

The objective of this work was to develop a novel composite absorbent from the two largest natural resources (α-cellulose and chitosan) with an ionic liquid as the medium in this study, explore its adsorption efficiency for CR dye removal on cellulose/chitosan beads and investigate the mechanism underpinning the adsorption process.

2. Experimental procedure

2.1. Materials

Chitosan with a molecular mass of 100 kDa and a degree of deacetylation of 90% derived from crab shells was/Co. Ltd (Hangzhou, China). Whatman No. 1 filter paper (Cst #1001055) was obtained from Sigma-Aldrich (St. Louis, MO, USA). The cellulose samples were prepared by tearing the filter paper into small pieces and drying them *in vacuo* at 80˚C for around 10 h before use. CR (AR grade) was provided by Aladdin Chemistry Reagent Co. Ltd (Shanghai, China) and used without further purification; 1-ethyl-3-methylimidazolium acetate ([Emim]Ac) with purity ≥97% was obtained from Lanzhou Institute of Chemical Physics, (Lanzhou, China). The herbs *Prunus cistena*, *Momordica grosvenori*, *Prunus mume*, *Polygonum multiflorum thunb* and *Lonicera japonica* were purchased from Dasenlin Pharmaceutical Co. (Guangzhou, China).

2.2. Preparation of cellulose/chitosan hydrogel beads

The cellulose/chitosan beads were prepared as presented in Fig. 1. Filter paper cellulose and chitosan were dispersed, respectively, in [Emim]Ac in an oil bath and stirred well at 70˚C to form a homogeneous solution with a concentration of 5% (w/w). The two solutions were then mixed together with different mass ratios at 70˚C and heated until a yellowish homogeneous liquid was formed. Using an Eppendorf 5-ml syringe tip, we extruded the mixture in droplet form, into a coagulating bath of absolute ethanol. We adjusted the height of the tip during manual operation to sit approximately 1–2 cm above the fluid surface to obtain beads which were as spherical as possible. Slow stirring overnight ensured complete coagulation. The spherical-shaped beads were collected by filtration and the filtrate was recycled by distillation under reduced pressure. The beads were washed and kept in deionised water to allow solvent exchange and produce hydrogel beads of cellulose/chitosan composite. The beads thus obtained were separated from the water, and then lyophilised until dry. The beads were stored in a desiccator at 25˚C.

2.3. Characterisation of cellulose/chitosan hydrogel beads

Both the specific surface area and pore size of the cellulose/chitosan hydrogel beads were measured by Brunauer–Emmet–Teller method. Samples were freeze-dried before analysis. Data were collected from pure liquid N_2 adsorption spectra at −196˚C using a JW-BK222 static nitrogen adsorption analyser [23].

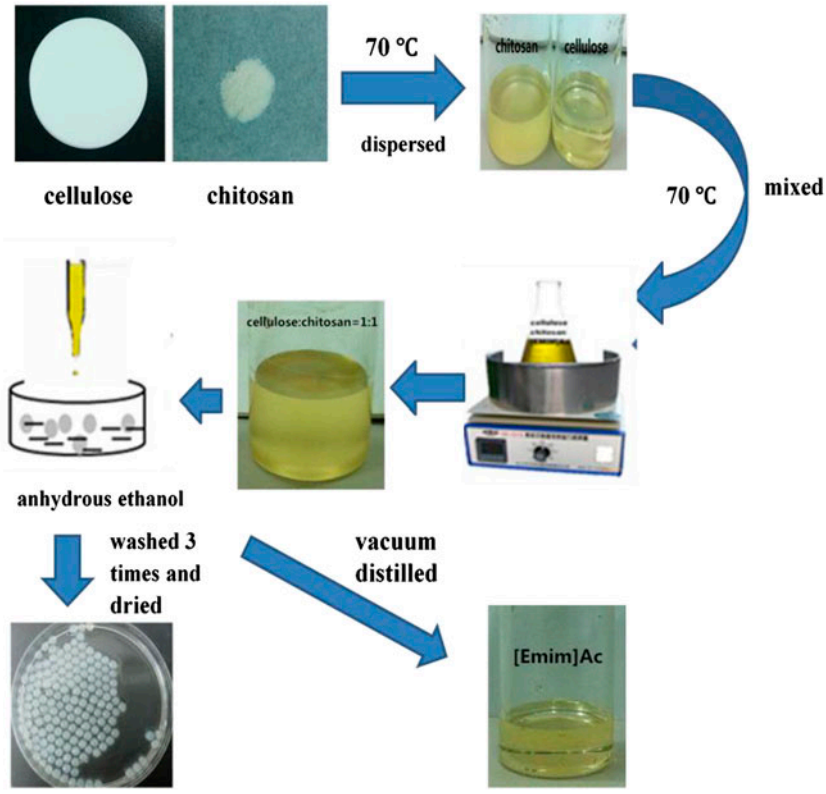

Fig. 1. Schematic illustration for the preparation of cellulose/chitosan hydrogel beads.

The infrared spectra of the cellulose/chitosan hydrogel beads, cellulose and chitosan were recorded using an FT-IR spectrometer (VECTOR 33) with a KBr pellet.

The X-ray powder diffraction (XRD) patterns of each raw material and the final product were measured by diffractometer (D8 ADVANCE) with Cu Kα X-ray radiation (λ = 0.15418 nm) under an accelerating voltage of 40 kV and a current of 40 mA. The scanning range was recorded from 5° to 60°, with an increment 2θ of 0.02° and 0.2 s per step.

The morphological features, surface characteristics and cross-sectional shape of the beads were obtained by SEM.

2.4. Adsorption of CR on cellulose/chitosan hydrogel beads

To prepare the standard curve of CR, absorbance of the tested samples was determined at CR concentrations of 10, 20, 30, 40, 50, 60 and 70 mg/mL by ultraviolet–visible spectrophotometer (λ_{max} = 498 nm).

Batch adsorption of CR on the cellulose/chitosan hydrogel beads was undertaken at 25℃ in a 100-ml flask, containing 50 ml of CR dye solution of known pH and concentration and a known mass of wet beads. The adsorption experiments on the cellulose/chitosan hydrogel beads were completed using a shaker table at a constant temperature of 25℃. Once in a while, the absorbance of the supernatant from the CR was determined by ultraviolet–visible spectrophotometer to allow calculation of its concentration. According to the concentration changes of the CR solution before and after adsorption, we calculated the amount of adsorption q_t (mg/g) and the percentage removal of CR dye.

$$q_t = (c_0 - c_t)V/M \quad (1)$$

$$\%\ \text{CR removal} = (c_0 - c_t)/c_0 \times 100\% \quad (2)$$

where c_0 and c_t (mg/L) denote the initial concentration and concentration of CR, respectively, at time t, M is the mass of adsorbent (g) and V (l) is the volume of the CR solution.

2.5. Decolourisation of traditional Chinese medicine (TCM) aqueous extract using cellulose/chitosan hydrogel beads

Traditional Chinese medicine (TCM) extracts from *P. cistena*, *M. grosvenori*, *P. mume*, *P. multiflorum thunb*

and *L. japonica* were prepared by refluxing the dried herbs with water (1:10, g/L) for 3 h at 90–100˚C. After removing the solid residue by filtration, the remaining aqueous extracts were subjected to decolourisation by putting the beads into TCM extracts, respectively, with the dosage of 0.5-g wet bead per 10-ml TCM extract and shaking at a constant temperature of 30˚C.

3. Results and discussion

3.1. Structural properties of cellulose/chitosan hydrogel beads

To enhance the mechanical strength of the cellulose/chitosan hydrogel beads, cellulose was blended into the chitosan. As the cellulose content increased, the shape of the cellulose/chitosan hydrogel beads became increasingly spherical and showed a denser structure than that of chitosan beads. However, increasing the chitosan content made it difficult to form spherical beads and caused cellulose/chitosan hydrogel beads to shrink. When the mass ratio of cellulose and chitosan was 1:1, the shapes and the mechanical strength of the cellulose/chitosan hydrogel beads were optimal. The mean size of the cellulose/chitosan hydrogel beads was about 3 mm. The average adsorption pore size of cellulose/chitosan hydrogel beads was 15.283 nm, meanwhile, the hydrogel bead specific surface area was 2.28377 m^2/g.

Fig. 2 shows the FT-IR adsorption spectra of the composite beads, the cellulose and the chitosan. As seen from Fig. 2, the characteristic peaks of cellulose/chitosan hydrogel beads corresponded to the characteristic peaks of cellulose and chitosan, it showed that the adsorption capacity of cellulose and chitosan remained. Cellulose/chitosan hydrogel beads, compared to the spectra of chitosan and cellulose, had an adsorption peak at 3,446 cm^{-1} which was significantly broadened: this was attributed to cross-linking between the hydroxyl groups of both cellulose and chitosan through hydrogen bonding. At 1,638 and 1,639 cm^{-1} bands indicative of the differences between chitosan and cellulose peaks were found: this was ascribed to a carbonyl group (amide I) and the N–H groups in the chitosan, respectively. For the cellulose/chitosan hydrogel beads, these two bands merged and shifted to 1,652 cm^{-1}. This indicated that the N–H groups of chitosan and their carbonyl groups interacted, thus proving that intermolecular interactions between cellulose and chitosan existed. Therefore, it can be concluded that the structure of cellulose and chitosan remained to a great extent; on the other hand, chemical cross-linking made a more stable structure therewith.

The XRD profiles of hydrogel beads are shown in Fig. 3. The characteristic reflections at $2\theta = 14.9^\circ$ and 22.8˚ indicated that the cellulose crystals were of the cellulose I type. The characteristic diffraction peak of chitosan at $2\theta = 10.7^\circ$ and 20.0˚. The diffracted intensity of the cellulose/chitosan hydrogel beads at $2\theta = 20.0^\circ$ decreased and there was no peak at 10.7˚. These results indicated that the crystal form of cellulose I was disrupted. It was because intermolecular and intramolecular hydrogen bonds of cellulose and chitosan were destroyed by ionic liquid. The formation of new hydrogen bond between cellulose and chitosan also lead to the destruction of the degree of crystallinity. The amorphous region increased after cellulose and chitosan were mixed.

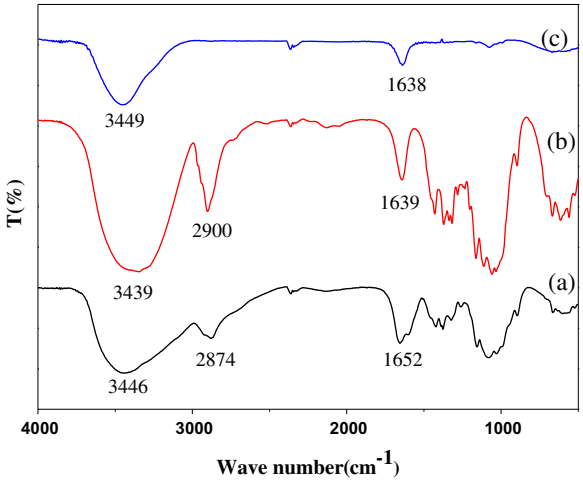

Fig. 2. FT-IR spectrum of: (a) cellulose/chitosan hydrogel beads, (b) cellulose powder and (c) chitosan powder.

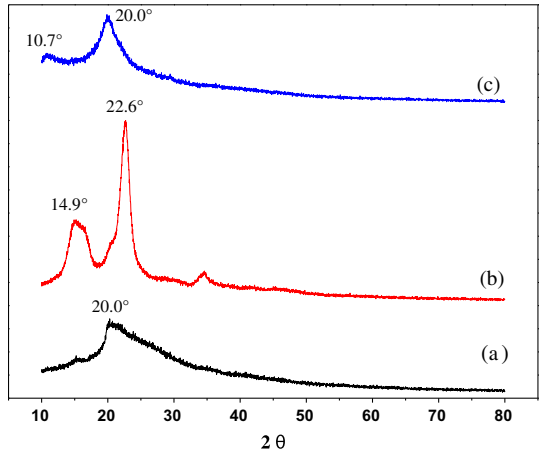

Fig. 3. XRD patterns of (a) cellulose/chitosan hydrogel beads, (b) cellulose powder and (c) chitosan powder.

Typical SEM images for cellulose/chitosan hydrogel beads are shown in Fig. 4(a)–(c). Fig. 4(a) shows the cellulose/chitosan hydrogel beads (50× magnification): each bead was coarse, contained deep surface ravines and had a structure that was easy to deposit during adsorption. Fig. 4(b) shows the rough, porous structure of the hydrogel bead surface. The cross-section of these cellulose/chitosan hydrogel beads, as shown in Fig. 4(c), further revealed the porous, rough structure. SEM images showed that the cellulose/chitosan hydrogel bead surface and cross-sections contained numerous holes and ravine structures which could provide many adsorption sites: this allowed fast channel, and CR dye diffusion, into these internal pores. This then allowed contact with the adsorption sites.

3.2. Effect of CR concentration

To investigate the effect of the original concentration of CR on the adsorption capacity of cellulose/chitosan hydrogel beads, four CR concentrations (10, 30, 50 and 70 mg/L), respectively, were selected. Fig. 5(a) shows that the adsorption rates were initially rapid because of the number of readily accessible sites: they subsequently became much slower. The percentage dye removal increased with increasing contact time (up to 600 min). As the initial CR concentration increased from 10 to 70 mg/L, the hydrogel beads exhibited a rapid decrease in CR removal efficiency from 92.7 to 46.7%, the equilibrium time, with the use of hydrogel beads, increased from 160 to 400 min. The high CR removal efficiency in the initial stages of the adsorption time corresponded to the large number of vacant adsorption sites. Initially, it is available for adsorption; however, because of the repulsive force between the solution phase and that CR absorbed on the surface of the hydrogel beads, the remaining available surface sites became increasingly difficult to occupy over time.

3.3. Effect of absorbent dosage

The results of CR (30 mg/L) removal at 0.2, 0.5, 1.0 and 2.0 g/L are shown in Fig. 5(b). The per cent CR removal and adsorption rate increased with an

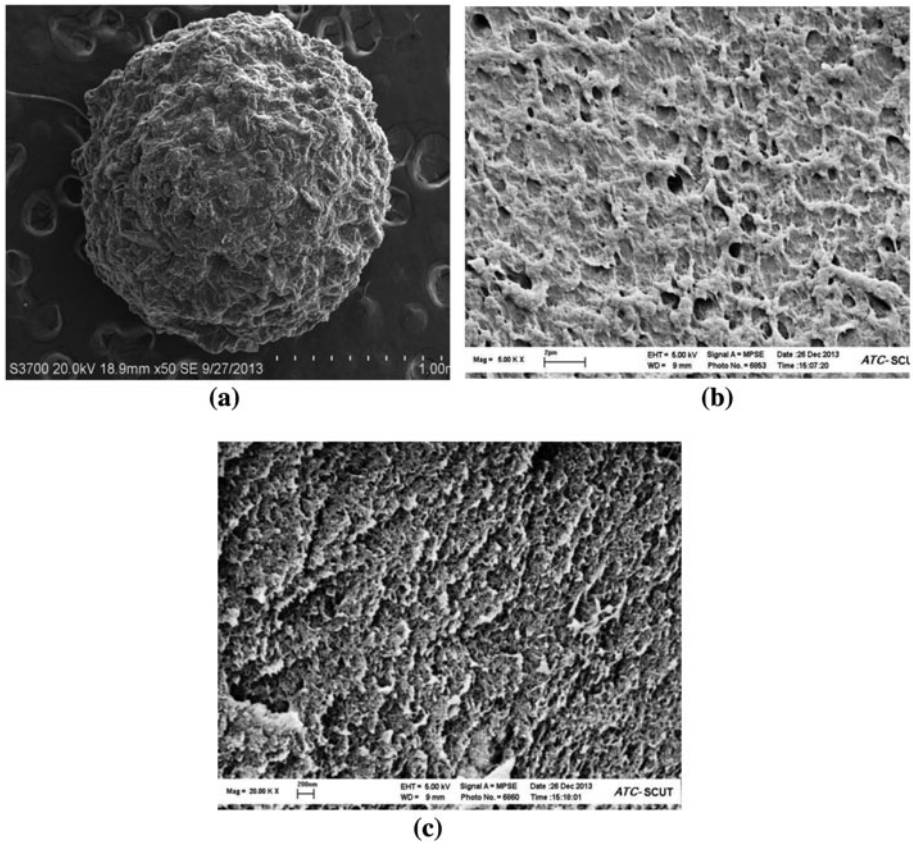

Fig. 4. SEM image of cellulose/chitosan hydrogel beads: (a) picture of hydrogel beads (50× magnification), (b) surface structure of hydrogel beads (5,000× magnification) and (c) cross-section of hydrogel beads (20,000× magnification).

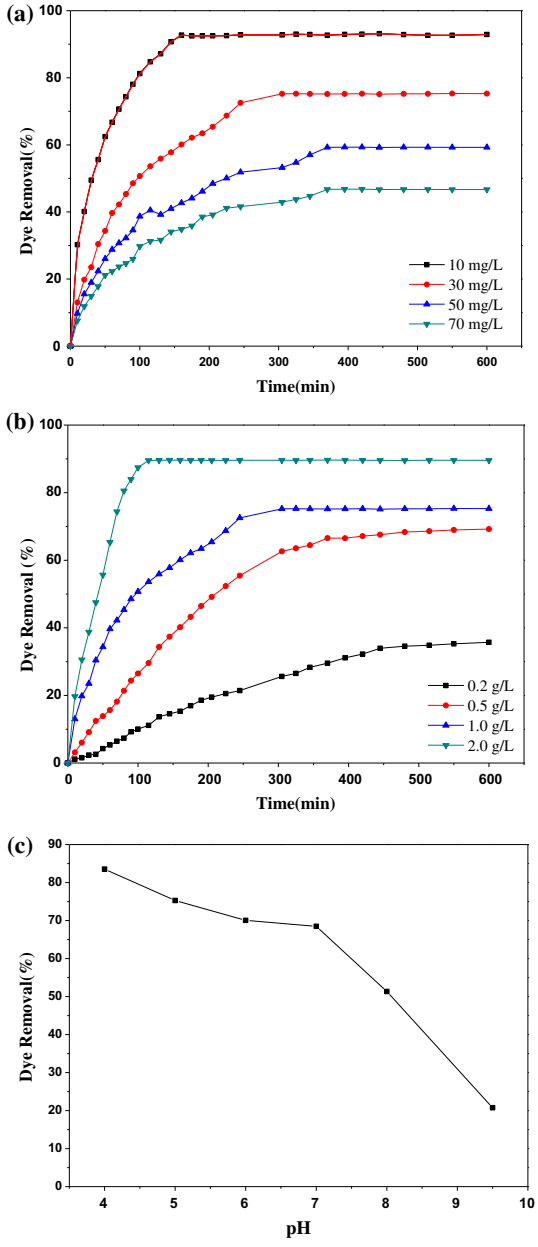

Fig. 5. Effect of (a) initial dye concentration, (b) adsorbent dosage and (c) initial pH on removal of CR on hydrogel beads.

increase in the absorbent dosage. For instance, the CR removal at equilibrium increased from 35.7 to 89.6% as the cellulose/chitosan hydrogel bead dosage increased from 0.2 to 2.0 g/L. The equilibrium time decreased from 550 to 115 min as the absorbent dosage increased. This adsorption process became easier because of an increase in the number of active adsorption sites and an increased surface area [24]. The result was consistent with the previous literature on CR removal [1].

3.4. Effect of pH

The influence of the original pH value on CR (30 mg/L) removal by a 1.0 g/L hydrogel bead dose is shown in Fig. 5(c). The CR removal efficiency was dependent on the original pH values of the CR dye solution. The percentage removal of CR decreased from 83.5 to 20.8% as the pH of the CR solution increased from 4.0 to 9.5. It was clear that the influence of pH on adsorption efficiency could be ascribed to a change in the surface electronic charge of the CR solution. CR molecules have two sulpho-groups: it was thus easily ionised in an acidic environment, and turned into a soluble anion. Then the CR anions can be easily adsorbed onto the positively charged surface of the adsorbent in either an acidic or neutral environment.

3.5. Adsorption kinetics

Several kinetic models were used to explain the adsorption behaviour including the pseudo-first-order model [25], pseudo-second-order model [26,27] and the Elovich and intraparticle diffusion equations. The pseudo-first-order and pseudo-second-order models are generally given as Eqs. (3) and (4), respectively:

$$\ln(q_e - q_t) = \ln q_e - k_1 t \tag{3}$$

$$t/q_t = 1/(k_2 q_e^2) + t/q_e \tag{4}$$

where q_e and q_t (mg/g) are, respectively, the amount of CR absorbed on the hydrogel beads at equilibrium and at time t (min), k_1 (min^{-1}) is the pseudo-first-order model rate parameter and k_2 (g/mg/min) is the pseudo-second-order model rate parameter.

The Elovich expression [28] is:

$$q_t = \frac{1}{b}[\ln(ab) + \ln t] \tag{5}$$

where a is the rate constant for the initial adsorption and b is the rate constant associated with surface coverage and chemical adsorption activation energy.

The intraparticle diffusion equation identified that intraparticle diffusion was the sole rate-limiting step in the adsorption of CR. The intraparticle equation of Weber and Morris is expressed [29] by:

$$q_t = k_i t^{0.5} + c_i \tag{6}$$

where k_i (mg/g $min^{-0.5}$) is the rate parameter for intraparticle diffusion and c_i (mg/g) is the intercept.

Fig. 6 shows the three kinetic models of CR adsorption on hydrogel beads. The experimental data and correlation coefficient (R^2) are summarised in Table 1. The kinetic data obtained from these three models are shown in Fig. 6. All linear forms were indeed linear regardless of initial CR concentrations. While, according to the values of R^2 for the three kinetic models given in Table 1, the experimental result was better fitted by the pseudo-second-order model. The calculated q_e values were similar to the experimental values, exhibiting a good linear relationship with a R^2 of above 0.99. The result therefore suggested that a pseudo-second-order model can represent the adsorption kinetic mechanism.

Adsorption plots at different initial concentrations are shown in Fig. 7. The absorption was almost proportional to $t^{0.5}$, but not to t. If the plot of q_t vs. $t^{0.5}$ was linear and passing through the origin, then intraparticle diffusion was the only rate-controlling step [30]. Fig. 7 shows that the plots of q_t vs. $t^{0.5}$ were non-linear, revealing that intraparticle diffusion rate was not the sole rate-controlling stage during adsorption. Multi-linearity was observed throughout the plot, which implied that the adsorption of CR solution on cellulose/chitosan hydrogel beads was governed by two steps. The original line segment was ascribed to CR diffusion in aqueous solution, which was governed by surface layer diffusion. This was related to the hydrogel bead structure. Subsequently, CR was transferred, and was adsorbed onto the inner surface of the cellulose/chitosan hydrogel beads in a gradual diffusion stage.

Table 2 shows the calculated values of k_i for four different initial concentrations. The intraparticle diffusion model fitted both the first and second linear stages.

3.6. Adsorption isotherm study

Both Langmuir and Freundlich isotherms were used to investigate the interaction between adsorbate molecular and absorbent surfaces.

The Langmuir isotherm model [29] assumed that the structure of the absorbent was homogeneous and was used successfully in monolayer absorption:

$$\frac{c_e}{q_e} = \frac{1}{q_e K_L} + \frac{c_e}{q_{max}} \quad (7)$$

where c_e (mg/L) is the equilibrium CR concentration, q_e (mg/g) is the equilibrium CR concentration on the absorbent, q_{max} is the maximum monolayer coverage adsorption capacity (mg/g) and K_L is the Langmuir parameter relating to the adsorption energy. The plot of c_e/q_e vs. c_e indicated a linear relationship, q_m and K_L can be obtained from the slope $1/q_{max}$ and intercept $1/(q_e K_L)$ thereof.

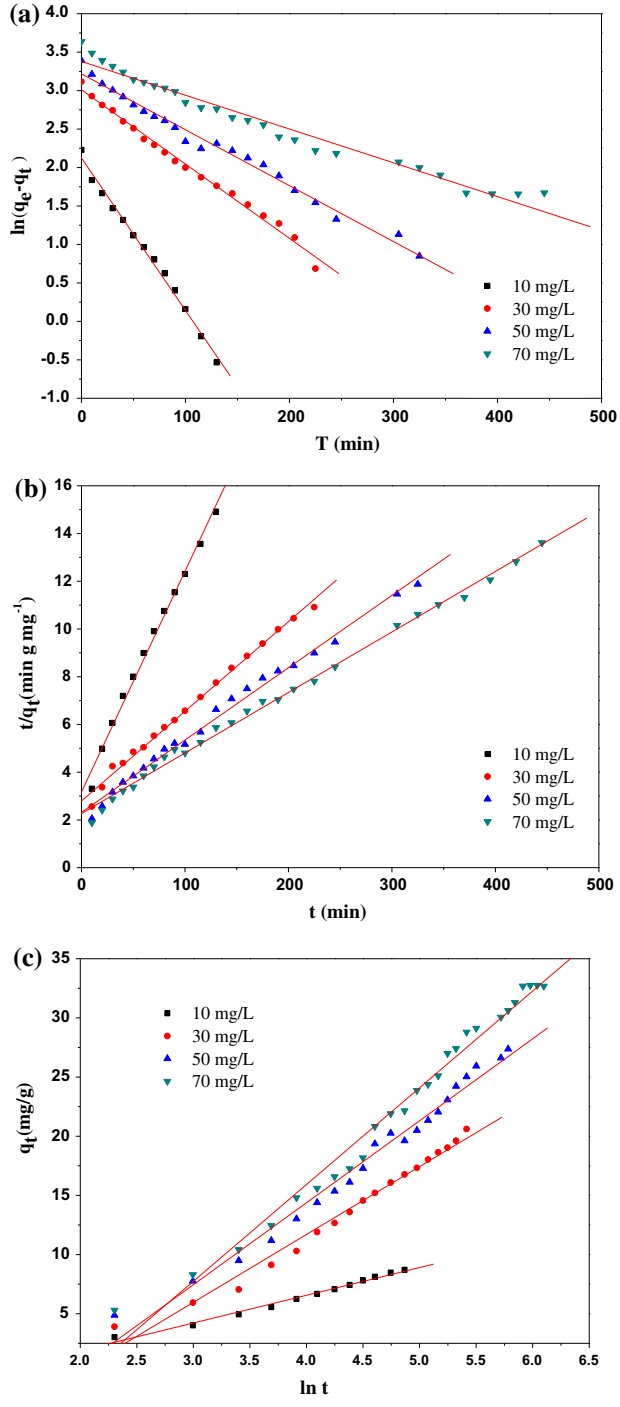

Fig. 6. Linear regressions of kinetic plots: (a) pseudo-first-order model, (b) pseudo-second-order model and (c) Elovich equation.

Table 1
Kinetic parameters for the adsorption of CR on cellulose/chitosan hydrogel beads

C_0		Pseudo-first-order model			Pseudo-second-order model			Elovich model		
(mg/L)	$q_{e,exp}$ (mg/g)	$q_{e,cal}$ (mg/g)	K_1 (min^{-1})	R^2	$q_{e,cal}$ (mg/g)	K_2 (min^{-1})	R^2	a (mg/g)	b (mg/g)	R^2
10	9.3	8.37	0.019	0.993	10.87	0.0027	0.991	0.705	0.427	0.987
30	22.6	20.31	0.009	0.991	27.03	0.00049	0.993	0.808	0.174	0.981
50	29.7	24.98	0.007	0.986	33.33	0.00039	0.991	1.01	0.144	0.981
70	38.0	29.34	0.004	0.968	40	0.00028	0.995	1.05	0.122	0.983

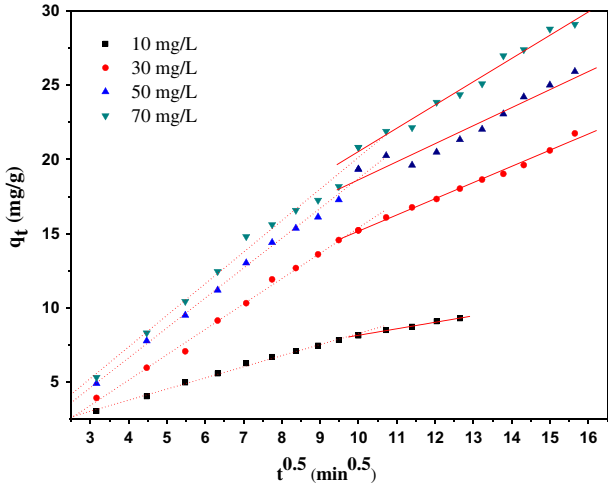

Fig. 7. Intraparticle diffusion model for adsorption of CR on hydrogel beads.

Table 2
Intraparticle diffusion model for CR adsorption on cellulose/chitosan hydrogel beads

	The whole processes		First stage		Second stage	
C_0 (mg/L)	k_i	R^2	$k_{i,1}$	R^2	$k_{i,2}$	R^2
10	0.664	0.984	0.750	0.996	0.437	0.994
30	1.394	0.983	1.712	0.995	1.093	0.990
50	1.630	0.980	2.017	0.994	1.217	0.940
70	1.914	0.991	2.131	0.987	1.570	0.982

The Freundlich isotherm model [31] was used to describe non-ideal adsorption on heterogeneous surfaces: it is not limited to monolayer formation. The linearised form of the Freundlich isotherm equation is:

$$\ln q_e = \ln K_F + \frac{1}{n} \ln c_e \quad (8)$$

where K_F ((mg/g) (L/mg)$^{1/n}$) is the Freundlich adsorption isotherm coefficient associated with the

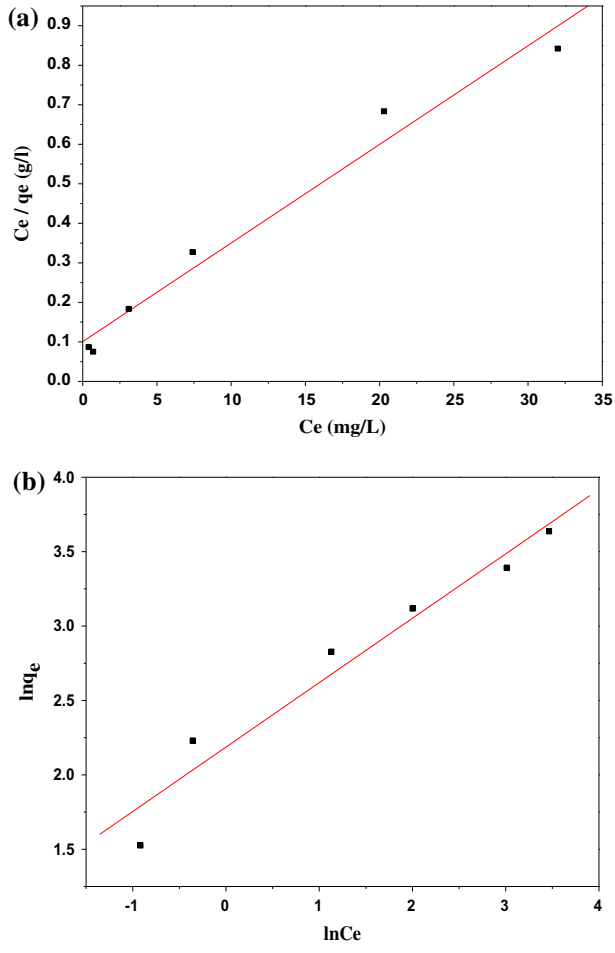

Fig. 8. Fit equilibrium data to linear (a) Langmuir isotherm model and (b) Freundlich model.

Table 3
Adsorption isotherm constants for CR adsorption on cellulose/chitosan hydrogel beads

	Langmuir constants			Freundlich constants		
T (K)	q_{max} (mg/g)	K_L	R^2	K_F	n	R^2
298	40	0.25	0.974	8.9	2.31	0.952

Table 4
q_{max} values for the adsorption of CR on different adsorbents

Type of adsorbent	q_{max} (mg/g)	Refs.
Cellulose/chitosan hydrogel beads	40	This study
Red mud	4.05	[34]
Kaolin	5.44	[23]
Coir pith	6.72	[36]
β-CD polymer	36.20	[35]
Acid-activated red mud	7.08	[37]
Chitosan beads	93.71	[33]
Chitosan/montmorillonite nanocomposite	54.52	[32]

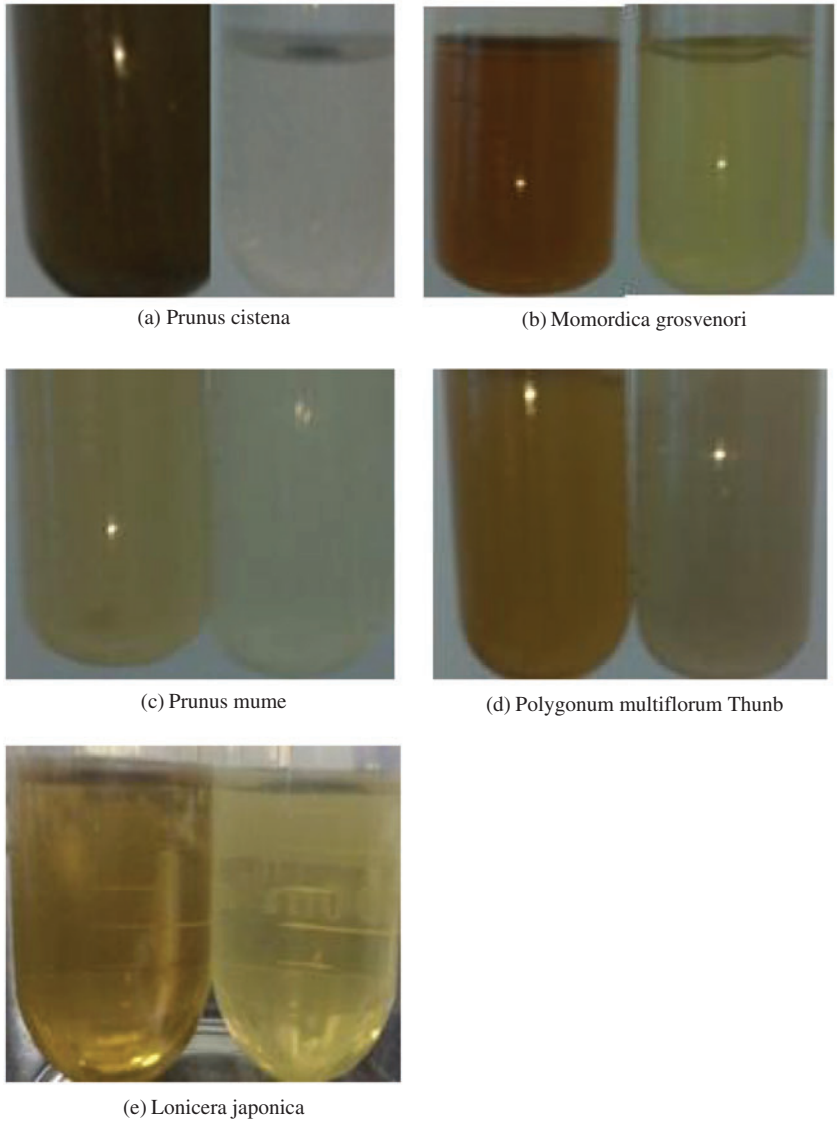

(a) Prunus cistena (b) Momordica grosvenori

(c) Prunus mume (d) Polygonum multiflorum Thunb

(e) Lonicera japonica

Fig. 9. Decolourisation of TCM aqueous extracts by cellulose/chitosan beads. Left: TCM aqueous extract before beads treatment; right: after treatment.

extent of the adsorption process and $1/n$ is an indicator of the favourability of sorption related to adsorption intensity. When $\ln q_e$ is plotted against $\ln c_e$, the constant K_F and indictor n are obtained.

Fig. 8(a) and (b) shows the linearised Langmuir and Freundlich isotherm plots at 25℃. The corresponding Langmuir and Freundlich isotherm data calculated from the linear plots are summarised in Table 3. Comparing the R^2 values of the linear form for both isotherm models, it may be seen that the Langmuir adsorption pattern was more consistent with the experimental results than the Freundlich isotherm. The maximum adsorption amount (q_{max}) of the hydrogel beads for CR obtained from the Langmuir equation was 40 mg/g, which was close to the experimental value of 38 mg/g. This proved that the CR chemical adsorption process was mainly a monolayer adsorption.

3.7. Comparison with other absorbents

The maximum CR adsorption amount (q_{max}) of different types of low-cost materials is listed in Table 4. Cellulose/chitosan hydrogel beads exhibited a relatively high adsorption capacity compared to some adsorbents. A higher q_{max} (54.52 mg/g) is achieved using a chitosan/montmorillonite nanocomposite [32], and the adsorption capacity of cellulose/chitosan hydrogel beads was much lower than that of chitosan beads [33]. Nevertheless, the q_{max} values of the cellulose/chitosan hydrogel beads were higher than those of red mud [34], kaolin [23], β-CD polymer [35], coir pith [36] and acid-activated red mud [37]. Therefore, since cellulose/chitosan hydrogel beads have comparable adsorption efficiency and were easy to recycle, they were considered a suitable adsorbent for CR removal from aqueous solutions. At the same time, their preparation was simple and eco-friendly.

3.8. Decolourisation of TCM aqueous extract using cellulose/chitosan hydrogel beads

Decolourisation of TCM has attracted growing interest in the pharmaceutical industry because the pigment not only affects the colour of the product but also inhibit the efficacy. At present, the general decolourisation was by column chromatography, the development of a new method of decolourisation is very important.

As shown in Fig. 9, the colour degree of *P. cistena*, *M. grosvenori*, *P. mume*, *P. multiflorum thunb and L. japonica* decreased significantly after hydrogel beads adsorption, which indicated that the pigment content was greatly reduced. This was ascribed to the large amounts of hydroxyl and amino of cellulose and chitosan of hydrogel beads. They can interact with the coloured impurities contained in the herbal extracts, and make it wrapped around cellulose and chitosan with linear molecular structure and then reach the effect of decolourisation. The numerous holes and ravine structures contained in cellulose/chitosan hydrogel bead surface and cross-sections could also provide many adsorption sites.

4. Conclusions

Cellulose/chitosan hydrogel beads were prepared by a simple method. They are considered to be an effective biosorbent for CR dye removal from effluents. The results showed that the CR dye adsorption process was related to original CR concentration, the dosage of cellulose/chitosan hydrogel beads and initial pH values. The adsorption process followed a pseudo-second-order model. Intraparticle diffusion modelling suggested that the adsorption of CR solution on cellulose/chitosan hydrogel beads was controlled by two stages and was not simply a rate-limiting step. The CR adsorption isotherm conforms to the Langmuir model and the amount of monolayer adsorption was found to be 40 mg/g at 25℃. Therefore, cellulose/chitosan hydrogel beads can be considered an efficient absorbent for CR dye removal from wastewater.

Acknowledgements

Financial support was provided by the National Natural Science Foundation of China (Grant numbers 31071505 and 31371743), and the Fundamental Research Fund for the Central Universities, SCUT (No. 2013ZZ078).

References

[1] Z. Hu, H. Chen, F. Ji, S. Yuan, Removal of Congo Red from aqueous solution by cattail root, J. Hazard. Mater. 173 (2010) 292–297.
[2] S. Wang, Removal of dyes from aqueous solution using fly ash and red mud, Water Res. 39 (2005) 129–138.
[3] S. Wang, Z. Zhu, Sonochemical treatment of fly ash for dye removal from wastewater, J. Hazard. Mater. 126 (2005) 91–95.
[4] B.K. Körbahti, Response surface optimization of electrochemical treatment of textile dye wastewater, J. Hazard. Mater. 145 (2007) 277–286.

[5] H. Zhu, R. Jiang, Y. Guan, Y. Fu, L. Xiao, G. Zeng, Effect of key operational factors on decolorization of methyl orange during H_2O_2 assisted CdS/TiO_2/ploymer nanocomposite thin films under simulated solar light irradiation, Sep. Purif. Technol. 74 (2010) 187–194.
[6] R. Jiang, H. Zhu, Y. Guan, Y. Fu, L. Xiao, Q. Yuan, S. Jiang, Effective decolorization of azo dye utilizing SnO_2/CuO/polymer films under simulated solar light irradiation, Chem. Eng. Technol. 34 (2011) 179–185.
[7] L. Lian, L. Guo, C. Guo, Adsorption of Congo red from aqueous solutions onto Ca-bentonite, J. Hazard. Mater. 161 (2009) 126–131.
[8] E. Bulut, M. Özacar, İ.A. Şengil, Equilibrium and kinetic data and process design for adsorption of Congo Red onto bentonite, J. Hazard. Mater. 154 (2008) 613–622.
[9] S. Chakraborty, M.K. Purkait, S. DasGupta, S. De, J.K. Basu, Nanofiltration of textile plant effluent for color removal and reduction in COD, Sep. Purif. Technol. 31 (2003) 141–151.
[10] S. Chatterjee, T. Chatterjee, S. Woo, Adsorption of Congo Red from aqueous solutions using chitosan hydrogel beads formed by various anionic surfactants, Sep. Sci. Technol. 46 (2011) 986–996.
[11] W.S. Wan Ngah, S. Fatinathan, Adsorption of Cu(II) ions in aqueous solution using chitosan beads, chitosan–GLA beads and chitosan–alginate beads, Chem. Eng. J. 143 (2008) 62–72.
[12] M. Dash, F. Chiellini, R.M. Ottenbrite, E. Chiellini, Chitosan-a versatile semi-synthetic polymer in biomedical applications, Prog. Polym. Sci. 36 (2011) 914–981.
[13] W.S. Wan Ngah, L.C. Teong, M.A.K.M. Hanafiah, Adsorption of dyes and heavy metal ions by chitosan composites: A review, Carbohydr. Polym. 83 (2011) 1446–1456.
[14] L. Jin, R. Bai, Mechanisms of lead adsorption on chitosan/PVA hydrogel beads, Langmuir 18 (2002) 9765–9770.
[15] D. Klemm, B. Heublein, H.P. Fink, A. Bohn, Cellulose: Fascinating biopolymer and sustainable raw material, Angew. Chem. Int. Ed. 44 (2005) 3358–3393.
[16] G. Annadurai, R.S. Juang, D.J. Lee, Use of cellulose-based wastes for adsorption of dyes from aqueous solutions, J. Hazard. Mater. 92 (2002) 263–274.
[17] S.J. Allen, Mass transfer processes in the adsorption of basic dyes by peanut hulls, Ind. Eng. Chem. Res. 44 (2005) 1942–1949.
[18] L. Zhang, J. Zhou, D. Zhou, Y. Tang, Adsorption of cadmium and strontium on cellulose/alginic acid ion-exchange membrane, J. Membr. Sci. 162 (1999) 103–109.
[19] D. Zhou, L. Zhang, J. Zhou, S. Guo, Development of a fixed-bed column with cellulose/chitin beads to remove heavy-metal ions, J. Appl. Polym. Sci. 94 (2004) 684–691.
[20] T.S. Anirudhan, S. Jalajamony, L. Divya, Efficiency of amine-modified poly(glycidyl methacrylate)-grafted cellulose in the removal and recovery of vanadium(V) from aqueous solutions, Ind. Eng. Chem. Res. 48 (2009) 2118–2124.
[21] N. Isobe, U.J. Kim, S. Kimura, M. Wada, S. Kuga, Internal surface polarity of regenerated cellulose gel depends on the species used as coagulant, J. Colloid Interface Sci. 359 (2011) 194–201.
[22] N. Isobe, M. Sekine, S. Kimura, M. Wada, S. Kuga, Anomalous reinforcing effects in cellulose gel-based polymeric nanocomposites, Cellulose 18 (2011) 327–333.
[23] V. Vimonses, S. Lei, B. Jin, C.W.K. Chow, C. Saint, Kinetic study and equilibrium isotherm analysis of Congo Red adsorption by clay materials, Chem. Eng. J. 148 (2009) 354–364.
[24] I.D. Mall, Removal of congo red from aqueous solution by bagasse fly ash and activated carbon: Kinetic study and equilibrium isotherm analyses, Chemosphere 61 (2005) 491–492.
[25] Y. Ren, X. Wei, M. Zhang, Adsorption character for removal Cu(II) by magnetic Cu(II) ion imprinted composite adsorbent, J. Hazard. Mater. 158 (2008) 12–14.
[26] Y.S. Ho, Review of second-order models for adsorption systems, J. Hazard. Mater. 136 (2006) 681–689.
[27] M. Ahmad, R.T. Bachmann, M.A. Khan, R.G.J. Edyvean, U. Farooq, M.M. Athar, Dye removal using carbonized biomass, isotherm and kinetic studies, Desalin. Water Treat. 53 (2015) 2289–2298.
[28] C.W. Cheung, J.F. Porter, G. McKay, Sorption kinetics for the removal of copper and zinc from effluents using bone char, Sep. Purif. Technol. 19 (2000) 54–55.
[29] J. Lin, Y. Zhan, Z. Zhu, Adsorption characteristics of copper(II) ions from aqueous solution onto humic acid-immobilized surfactant-modified zeolite, Colloids Surf., A 384 (2011) 6–9.
[30] Y.S. Ho, G. McKay, Sorption of dyes and copper ions onto biosorbents, Process Biochem. 38 (2003) 1047–1061.
[31] D. Liu, D. Sun, Y. Li, Removal of Cu(II) and Cd(II) from aqueous solutions by polyaniline on sawdust, Sep. Sci. Technol. 46 (2010) 321–329.
[32] L. Wang, A. Wang, Adsorption characteristics of Congo Red onto the chitosan/montmorillonite nanocomposite, J. Hazard. Mater. 147 (2007) 979–985.
[33] S. Chatterjee, S. Chatterjee, B.P. Chatterjee, A.K. Guha, Adsorptive removal of congo red, a carcinogenic textile dye by chitosan hydrobeads: Binding mechanism, equilibrium and kinetics, Colloids Surf., A 299 (2007) 146–152.
[34] C. Namasivayam, D.J.S.E. Arasi, Removal of congo red from wastewater by adsorption onto waste red mud, Chemosphere 34 (1997) 401–417.
[35] E.Y. Ozmen, M. Yilmaz, Use of β-cyclodextrin and starch based polymers for sorption of Congo red from aqueous solutions, J. Hazard. Mater. 148 (2007) 303–310.
[36] C. Namasivayam, D. Kavitha, Removal of Congo Red from water by adsorption onto activated carbon prepared from coir pith, an agricultural solid waste, Dyes Pigm. 54 (2002) 47–58.
[37] A. Tor, Y. Cengeloglu, Removal of congo red from aqueous solution by adsorption onto acid activated red mud, J. Hazard. Mater. 138 (2006) 409–415.